Decay of 92.5-Min La^{142}†

W. V. Prestwich and T. J. Kennett
McMaster University, Hamilton, Ontario, Canada
(Received 9 December 1963; revised manuscript received 11 February 1964)

The decay properties of 92.5-min La^{142} have been studied using scintillation spectrometric techniques. The energies, intensities, and time-correlations of the associated beta and gamma transitions have been investigated. The gamma-ray energies (and relative intensities) observed are: 0.645 (1.000), 0.86 (0.05), 0.898 (0.185), 1.01 (0.094), 1.06 (0.077), 1.16 (0.059), 1.25 (0.057), 1.37 (0.050), 1.55 (0.053, 0.044), 1.74 (0.106), 1.91 (0.176), 2.06 (0.132), 2.14 (0.044), 2.19 (0.099), 2.41 (0.314), 2.55 (0.227), 2.67 (0.061), 2.80 (0.046), 2.99 (0.11), 3.14 (0.021), 3.31 (0.039), 3.45 (0.026), 3.65 (0.048) MeV. The beta-ray groups (and approximate branching ratios) are 4.49 (13%), 3.85 (2%), 2.98 (2%), 2.31 (7%), 2.11 (24%), 1.98 (20%), 1.79 (11%), 1.23 (5%), 0.87 (13%) MeV. On the basis of these results, a decay-scheme has been constructed with excited states in Ce^{142} at 0.645, 1.54, 1.66, 2.02, 2.19, 2.41, 2.55, 2.71, 3.31, 3.45 and 3.65 MeV. The Q_β value for the La^{142}–Ce^{142} decay was found to be 4.51±0.03 MeV.

1. INTRODUCTION

THE properties of the nuclei in the transition region, between the closed-shell and well-deformed configurations, are particularly interesting in that they exhibit the interplay between collective and intrinsic dynamical modes. A study of the level structure of even-even transition nuclei should lead to information about the extent to which these motions are separable. Deviations from adiabatic approximations may assume significance within the context of the microscopic description of nuclear dynamics advocated by Brown[1] and Mottelson[2] and others.

Such transition nuclei in the region between $N=82$ and 90 are produced in relatively high yield in the thermal neutron fission of U^{235}. The Ce^{142} nucleus, adjacent to the $N=82$ closed shell, is such a transition nucleus. Previous researchers[3,4] have investigated the gamma-ray spectrum, the Q_β value, and a portion of the γ-γ coincidence matrix. In this work, the level structure of Ce^{142} is determined by a study of the decay of La^{142} using scintillation spectrometer techniques. It is hoped that these results will contribute to the systematics of level structure in this region.

2. EXPERIMENTAL TECHNIQUES

2.1 Preparation of La^{142} Samples

Uranium samples consisting of 100–300 μgm of U^{235} as the nitrate in 3-ml aqueous solutions were irradiated in polyethylene capsules for 1–4 min using the pneumatic system of the McMaster Nuclear Reactor. The flux at this position was 3×10^{12} neutrons/cm^2 sec. The sample was delivered to the receiving station approximately 10 sec after the end of the irradiation.

The initial step of the procedure, carried out 2 min after the end of the irradiation, was the separation of radiobarium from the gross fission products. The radiobarium was exchanged with 50 mg of barium carrier in the form of freshly precipitated barium chloride in 30 ml of concentrated HCl. The solution was filtered over a membrane filter and the precipitate washed with 30 ml of concentrated HCl. The precipitate was then dissolved in approximately 15 ml of water. From this point on, one of two methods was used to separate radiolanthanum from the barium solution.

Method 1: Since the most likely contaminant to be carried along with the fission-product barium is strontium, the precursor of yttrium, a lanthanum-yttrium separation using a tributyl-phosphate solvent extraction was used.[5] Ten milligrams of lanthanum carrier in the form of $La(NO_3)_2$ solution was added to the barium sample. Approximately 40 min after the end of the irradiation, lanthanum hydroxide was precipitated and the precipitate centrifuged. The precipitate was dissolved in concentrated HNO_3 and the solution agitated together with 10 ml of freshly pre-equilibrated tributyl phosphate (TBP). The lanthanum, which remains in the aqueous phase, was withdrawn into fresh TBP and the extraction repeated. The sample was obtained in its final form by precipitating lanthanum oxalate. The physical form of sources obtained in this procedure was a relatively uniform disc of lanthanum oxalate $\frac{1}{2}$ in. in diameter backed by filter paper.

Method 2: The method described above resulted in lanthanum separations with a radiochemical decontamination factor of at least 10^6. However, the total time required for the separation was approximately $1\frac{1}{2}$ hours. Also, the source thickness of 10 mg/cm^2 was considered relatively thick for some applications. For these reasons, a method resulting in a carrier-free sample a few minutes after the beginning of the lanthanum separation was investigated and proved highly satisfactory.[6] Forty minutes after the end of the irra-

† This work was financially supported by the National Research Council of Canada.

[1] G. E. Brown, J. A. Evans, and D. J. Thouless, Nucl. Phys. **24**, 1 (1961).

[2] B. R. Mottelson in *Proceedings of the International Conference on Nuclear Structure, Kingston Ontario, 1960* (The University of Toronto Press, Toronto, 1960), p. 525.

[3] R. P. Schuman, E. H. Turk, and R. L. Heath, Phys. Rev. **115**, 185 (1958).

[4] H. Ryde and C. J. Herrlander, Arkiv Fysik **13**, 177 (1958).

[5] K. Fritze and T. J. Kennett, Phys. Rev. **127**, 1262 (1962).

[6] J. E. Duval and M. H. Kurbatov, J. Am. Chem. Soc. **75**, 2246 (1953).

diation, concentrated ammonium hydroxide was added to the solution without the addition of lanthanum carrier. When passed over a membrane filter, the radiolanthanum was retained on the filter, presumably in the form of a colloid. It is not known whether the source forms a surface layer of is impregnated throughout the filter. In the latter case, the source thickness would be that of the filter paper, approximately 3 mg/cm^2.

2.2 Instrumentation

The scintillation γ-ray spectrometer used in this work consisted of a 3×3-in. NaI(Tl) crystal integrally mounted to a DuMont-6363 photomultiplier. The detector pulses were formed in a charge-sensitive preamplifier, amplified in a transistorized DD2 amplifier and analyzed in a 256-channel multichannel analyzer. For the single-crystal γ-ray spectrum a standard 10-cm geometry was used. The crystal face was covered with a 3-g/cm^2 polyethylene absorber.

For coincidence studies, two such detector-amplifier systems were used in conjunction with a multiple coincidence circuit. Timing markers for the coincidence circuit are formed using standard cross-over gates. The system was operated at a resolving time of $2\tau=50$ nsec. The coincidence distributions were analyzed using a standard fast-slow gating arrangement coupled to the one-dimensional analyzer. Specific energy regions were also examined using a two-dimensional 1024-channel analyzer in either 32×32 or 16×64 memory configurations. The detectors were arranged at 180° with a source-to-detector distance of 3 cm. The source was mounted in a 1-cm-thick lead anti-Compton shield.

The gamma-ray spectrum in the energy region above approximately 1.5 MeV was also investigated using a three-crystal pair spectrometer. The central detector was a $1\frac{1}{2}$×2-in. NaI(Tl) crystal mounted on a DuMont-6292 photomultiplier. Two 3-in. detectors were placed at either side of the center crystal and were shielded from direct source radiations by 2 in. of lead. A 3-in.-thick lead collimator with a $\frac{1}{2}$-in. aperture was placed between the source and the center crystal. Windows 0.06 MeV wide centered at 0.511 MeV were set on the outputs of the two side detectors. The output of the center crystal was analyzed in the one-dimensional analyzer gated by triple-fast coincidences satisfying the pulse-height condition required by the window settings.

The scintillation beta detector assembly consisted of a 2×2-in. NE-102 plastic phosphor optically coupled to an E.M.I.-9536 phototube. Spectra observed with this detector were corrected for finite response using the method of Freeman *et al.*[7] In addition, the single-crystal beta spectrum was observed with an anticoincidence arrangement in which partial-energy transfer events are suppressed. The arrangement is described in detail elsewhere.[8]

3. EXPERIMENTAL RESULTS

3.1 Energy and Intensity of Gamma-Ray Transitions

A relatively complete catalogue of the gamma-ray transitions which occur in the beta decay of 92.6-min La^{142} was obtained by considering the results of many experiments. These include the single-crystal gamma-ray spectrum, the three-crystal pair spectrum, and the coincidence spectra measured for several window settings.

The single-crystal gamma-ray spectrum of La^{142} is shown in Fig. 1. The Gaussian full-energy peaks of the spectral components of the spectrum are also shown. In order to avoid confusion the partial-energy portion of the response to each gamma ray has been omitted. The line shapes used for the analysis of spectra observed over the complete energy range were obtained from a library of standards.

Secondary internal calibration lines were determined using the method of mixed sources. A La^{142}–Na^{22} mixture was used to obtain the energies of the prominent lines in the region between 0.511 and 1.27 MeV. A La^{142}–Na^{24} mixture was used for the region between 1.3 and 2.8 MeV. As can be seen from Fig. 1, the spectrum is complex and exhibits a strong line at 0.645 MeV. This line, together with the less prominent lines at 1.91, 2.41, and 2.55 MeV were adopted as secondary standards. The positions of the secondary standards were determined by calculating the centroids of the full-energy peaks. The gain and zero-energy channel were considered as parameters of a linear pulse-height-energy, or dispersion, relation and their best values obtained from the internal standards by the method of least squares. A comparison of the values obtained in this manner indicated that over the energy range of 0.6–3.0 MeV, the neglect of the nonlinearity in the pulse-height-energy relation introduces an error of less than 0.2%. The error is, of course, mainly absorbed in the zero-channel parameter and the method would not be as accurate in the energy region below approximately 0.5 MeV where the nonlinearity is more serious. The accuracy with which the position of the full-energy peak can be determined depends upon the magnitude of the interfering contributions from partial-energy events corresponding to higher energy gamma rays. The energies of the remaining gamma rays in the spectrum were determined using the positions of the full-energy peaks of the analyzed components and the fitted dispersion relation. In this manner the energies were recalculated in each experiment. In this way the experi-

[7] M. S. Freedman, T. B. Novey, F. T. Porter, and F. Wagner, Jr., Rev. Sci. Instr. **27**, 716 (1956).

[8] T. J. Kennett and G. L. Keech, Nucl. Instr. Methods **24**, 142 (1963).

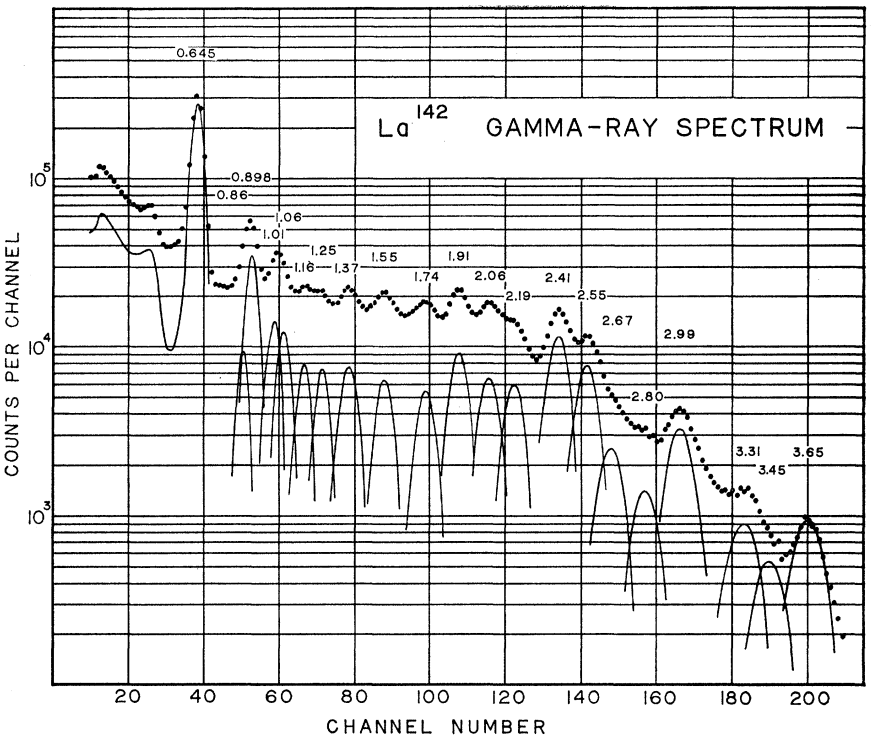

FIG. 1. Single-crystal gamma-ray spectrum of La^{142}, observed with a 3×3-in.-NaI(Tl) detector. The face of the crystal was covered with a 4-g/cm² polyethylene beta absorber. The source-detector distance was 10 cm. The spectrum is shown analyzed into single-line components for which only the full-energy peaks are indicated.

ments were checked for consistency and the values obtained were averaged with the existing values.

Unfortunately, it was impossible to obtain standard line shapes corresponding to incident gamma-ray energies greater than 3.1 MeV. It was necessary to construct line shapes for the analysis of this energy region of the La^{142} spectrum by extrapolation. The contribution from summing was measured for the 10-cm geometry using the method discussed by Johnson *et al.*[9] The sum contribution was never greater than 5% of the gross spectrum so that the subtraction of this contribution introduced a negligible uncertainty. As can be seen from Fig. 1, there is a departure of the data on the high-energy side of the 3.65-MeV full-energy peak. Although this line shape was based on an extrapolation procedure, it is felt that the error in the response is small compared to the observed deviation. However, since the existence of any transition of energy greater than 3.65 MeV was not revealed in the course of this study, it is concluded that a small residual remains.

A residual in the region of 3.1 MeV revealed the existence of a weak transition at this energy. However, it was not possible to obtain sufficient information about the transition to include it in the decay scheme. The existence of the 2.67-MeV gamma ray, revealed in the stripping, was first suggested by Schumann *et al.*[3] and confirmed in this investigation by coincidence results. Other evidence which will be cited later also confirmed the existence of all the components shown in Fig. 1 which were revealed by graphical analysis. The analysis of the 1.01–1.05- and 0.86–0.898-MeV doublets were particularly difficult. Initially it was merely noted that the widths of these lines were somewhat broadened. The lower energy region of the spectrum was analyzed separately using the distribution measured with a higher gain. In this case, the required line shapes were obtained from measurements of the spectra of Cs^{137} (0.662 MeV), Mn^{54} (0.835 MeV) and Zn^{65} (1.114 MeV) performed immediately after the run so that similar counting conditions applied. The contribution from higher energy gamma rays was calculated on the basis of the analysis of the spectrum in Fig. 1. Careful graphical analysis of the high-gain spectrum lead to the relative contributions for the components of these doublets as shown in Fig. 1.

The relative intensity of each component of the spectrum was calculated using the area of the full-energy peak corrected for photoefficiency. The correction factors given by Heath[10] were used. Except in the region of 1.37 MeV, all portions of the spectrum were observed to decay with the 92.6-min half-life corresponding to La^{142}. The 1.37-MeV transition was found to consist of approximately equal contributions of 92.6-min La^{142} and 3.7-h La^{141} over the counting period used.

Using a design matrix based upon the results of the graphical analysis, the spectrum was analyzed by the

[9] N. R. Johnson, E. Eichler, G. D. O'Kelley, J. W. Chase, and J. T. Wasson, Phys. Rev. **122**, 1546 (1961).

[10] Nuclear Data Group, National Academy of Science—National Research Council, Washington, D. C.

method of multiple linear regression. The regression values, the corresponding variance-covariance matrix and the variance ratios were determined. The variance ratios indicated that each component (including the 3.1-MeV line) was statistically significant, exceeding the 95% confidence limit. Of course, the existence of a residual not taken into account in the design matrix would invalidate definite conclusions based on the variance ratios. The differential residual indicated no significant trends and the effective value of χ^2/f for the model used was 1.8. This rather large value is believed to be caused mainly by inaccuracies in the line shapes and especially in the positioning of the full-energy peaks in the region between 1 and 2 MeV. The results obtained by graphical analysis and linear regression are shown in Table I. Except for the less prominent lines, the results of the two methods agree within 15% and usually within the standard deviation.

As mentioned above, the existence of weak transitions, though confirmed statistically, was still considered tentative until further experimental evidence was obtained. One source of such evidence concerning the transitions in the region above approximately 1.5 MeV is the three-crystal pair spectrum shown in Fig. 2.

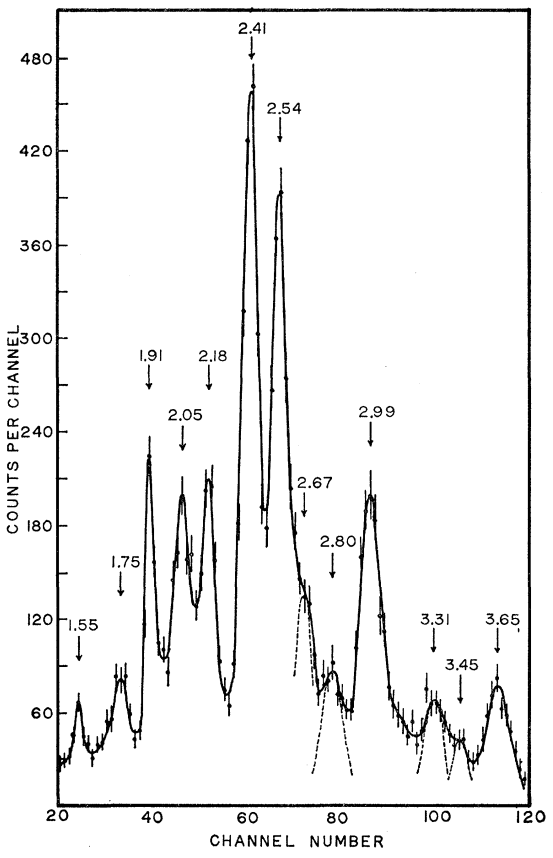

FIG. 2. Three-crystal pair spectrum of La^{142}. In this spectrum the transitions at 3.45, 2.80, 2.67, and 2.18 MeV are more clearly revealed than in the single-crystal spectrum of Fig. 1.

Because of the superior resolution and the simplified response, the more obscure transitions in the single-crystal spectrum are more clearly revealed. A definite peak is seen at 2.80 MeV. The 2.67-MeV line appears just barely resolved on the high-energy side of the 2.54-MeV peak. Because of the low intensity, the 3.45-MeV line is still not very prominent, but its existence is indicated.

The residual on the high-energy side of the 2.99-MeV peak also indicates the possible existence of the transition at 3.1 MeV referred to above. The peaks corresponding to the 2.05- and 2.18-MeV transitions are clearly resolved, in contrast to the corresponding peaks in the single-crystal spectrum. However, the valley between these two peaks is higher than expected on the basis of the resolution and energy separation indicating the possible existence of a weak transition at 2.1 MeV. The energies of the gamma transitions revealed in the three-crystal pair spectrum were found to agree with the corresponding energy values determined from the single-crystal spectrum within the experimental error of 1%. The intensities of the transitions relative to that of the 2.41-MeV transition were obtained by determining the peak areas corrected for the pair-production cross section. The values obtained are compared to the single-crystal values in Table I. Also shown in the table are the intensity measurements obtained from coincidence studies. These measurements are based on an interpretation of the coincidence quotients within the context of the proposed decay scheme.

3.2 Gamma-Gamma Coincidence Studies

Coincidence spectra were observed with the fast-slow coincidence spectrometer and the two-dimensional analyzer. Only the spectra obtained with the fast-slow system are shown in the illustrations. Each of these spectra was analyzed graphically to obtain the coincidence quotient q_{ij} defined by the expression.

$$q_{i,j}=\frac{1}{D_i}\left\{\frac{P_j e^{\mu d}}{C_w \mathcal{E}_j}-\sum_n D_r q_{rj}\right\}.$$

In the above expression P_j is the area of the photopeak γ_j, $e^{\mu d}$ and $\mathcal{E}_j$ are corrections for absorption and photofraction respectively, C_w is the number of counts in the window, and the D_r is the relative contributions of γ_r to the window. The second term in the expression represents the interference from higher energy gamma rays which give use to events in the window set on the photopeak of γ_i. The results obtained with the two-dimensional system were in agreement with those obtained with the fast-slow system. The results quoted are the averages of several experiments.

The spectrum shown in Fig. 3 is the distribution of events in coincidence with gating events selected by a window 0.05 MeV wide centered at 0.645 MeV. Events in this region correspond primarily to the 0.645-MeV

TABLE I. Summary of La^{142} gamma-ray transitions.

E_γ (MeV)	Relative intensity: Graphical analysis	Regression analysis	Pair spectrometer	Coincidence	Average
0.645±0.007	1.000	1.000			1.000
0.86 ±0.01	0.049	0.056±0.006		0.044	0.050
0.898±0.009	0.19	0.194±0.006		0.17	0.185
1.01 ±0.01	0.10	0.091±0.005		0.090	0.094
1.06 ±0.01	0.085	0.076±0.007		0.071	0.077
1.16 ±0.01	0.066	0.060±0.012		0.051	0.059
1.25 ±0.01	0.064	0.060±0.015		0.048	0.057
1.37 ±0.01	0.039	0.049±0.004		0.063	0.050
1.55 ±0.02	0.081	0.100±0.004	0.11	0.055,0.045	0.053,0.044
1.74 ±0.02	0.097	0.107±0.004	0.12	0.101	0.106
1.91 ±0.17	0.17	0.171±0.005	0.21	0.151	0.176
2.06 ±0.02	0.13	0.137±0.004	0.15	0.11	0.132
2.14 ±0.04	0.15	0.130±0.004	0.15	0.04	0.044
2.19 ±0.02				0.09	0.099
2.41 ±0.02	0.31	0.318±0.006	0.318[a]		0.314
2.55 ±0.02	0.22	0.229±0.005	0.23		0.227
2.67 ±0.03	0.06	0.073±0.004	0.07	0.040	0.061
2.80 ±0.03	0.05	0.044±0.003	0.05	0.039	0.046
2.99 ±0.03	0.12	0.130±0.003	0.10	0.091	0.11
3.14 ±0.04		0.031±0.004	0.02		0.026
3.31 ±0.03	0.04	0.038±0.003	0.04		0.039
3.45 ±0.03	0.03	0.029±0.002	0.02		0.026
3.65 ±0.04	0.05	0.054±0.002	0.04		0.048

[a] The relative intensity of this line was normalized to the corresponding single-crystal value.

transition. The coincidence spectrum obtained extends to the line at 2.99 MeV. Analysis revealed the existence of the 2.80- and 2.67-MeV lines. The region between 2.2 and 2.5 MeV was not entirely accounted for by the response to these three gamma rays, but because of the expected higher levels of interference, the residual was not considered to definitely indicate the existence of gamma transitions in this region. The energy of the transition at 2.14 MeV was consistently observed to be lower than the corresponding transition at 2.18 MeV present in the single-crystal and pair spectra. This result, together with the anomalous residual at 2.1 MeV in the pair spectrum, is believed to indicate that the transition at this energy is complex. The coincidence-quotient analysis indicates that approximately 60% of the transitions at this energy are in coincidence with

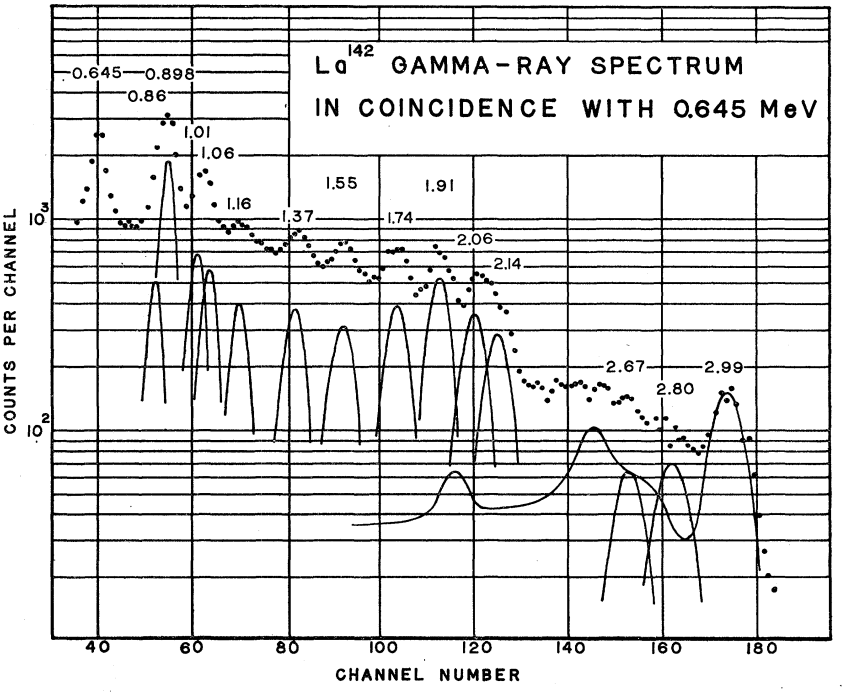

FIG. 3. Pulse-height distribution obtained in coincidence with gating events selected by a 0.05-MeV window centered at 0.645 MeV.

events in the window. Below 2 MeV, the spectrum is similar to the single-crystal gamma-ray spectrum. However, only 45% of the transitions at 1.54 MeV and 63% of the transitions at 1.37 MeV appear in coincidence with the 0.645-MeV gamma ray. As mentioned above, the 1.37-MeV line is attributable to both La^{142} and La^{141}, so that this result indicates that approximately 37% of the transitions at this energy in the spectrum shown in Fig. 1 are due to La^{141}. Further evidence from the coincidence experiments indicates that the 1.54-MeV peak corresponds to two unresolved gamma rays. The 0.645-MeV line which appears in the spectrum is caused by events in the gate corresponding to higher energy gamma rays.

The interference from such events was both treated analytically and measured experimentally. In the latter case, windows were set both at 0.645 and 0.76 MeV. Both distributions were sampled concurrently and routed into different subgroups of the analyzer memory. There was no significant difference between the results obtained experimentally and analytically.

The low-energy region of this spectrum was also investigated experimentally using a higher gain. Line shapes measured immediately after the run were used to analyze the spectrum. In agreement with the single-data, the analysis revealed the complex nature of the 1.01–1.06- and 0.860–0.898-MeV doublets.

In Fig 4 is shown the spectrum obtained for a window position of 0.88 MeV and width 0.05 MeV. Only 50% of the gating events at this position correspond to the gamma rays of interest, 0.860–0.898 MeV. The spectrum is characterized by an enhancement of the 1.16-MeV line and a broadening of the 0.860–0.898-MeV doublet. The previous authors (Refs. 3 and 4) suggested that the 1.0-MeV line was in coincidence with the 0.898-MeV transition. However, the coincidence quotient $q_{0.898,1.0}$ is nearly zero so that the appearance of the 1.0-MeV line in this spectrum is due to Compton interference. This result was confirmed in the corresponding two-dimensional distribution. The coincidence quotients for the 0.860–0.898-MeV doublet indicate that these transitions are members of a cascading pair. There is a considerable residual in the region above 1 MeV. The coincidence quotient for the 1.55-MeV peak, taken to be correlated with the 0.860-MeV component of the window, accounts for the 55% portion not in coincidence with the 0.645-MeV transition. The doublet at ~2 MeV accounts for approximately 30% of the single-crystal intensity.

In Fig. 5 is shown the coincidence spectrum obtained when a region of 0.05 MeV centered at 1.03 MeV is selected for gating. The gating fractions $D_{1.01}$ and $D_{1.06}$ are 25% and 24%, respectively. The most prominent feature of the spectrum is the enhancement of the 1.0–1.06-MeV doublet. The 0.898-MeV line is suppressed and the small coincident quotient confirms the fact that the major part of the 0.898- and 1.03-MeV transitions are not correlated. As in the case of the 0.898-MeV coincidence spectrum, there is a considerable residual above 1.2 MeV, only a part of which can be accounted for by the response to the 2.06-MeV gamma ray. The coincidences at 2.06 MeV comprise approximately 30% of the corresponding single-crystal intensity. In Fig. 6 is shown the low-energy region of this spectrum observed at higher gain. The analysis was based on the appropriate line shapes measured immediately after the run. The results confirm the doublet nature of the 1.03-MeV peak. The relative contributions of the 1.01- and 1.06-MeV components obtained in this analysis differ from the corresponding results obtained in the

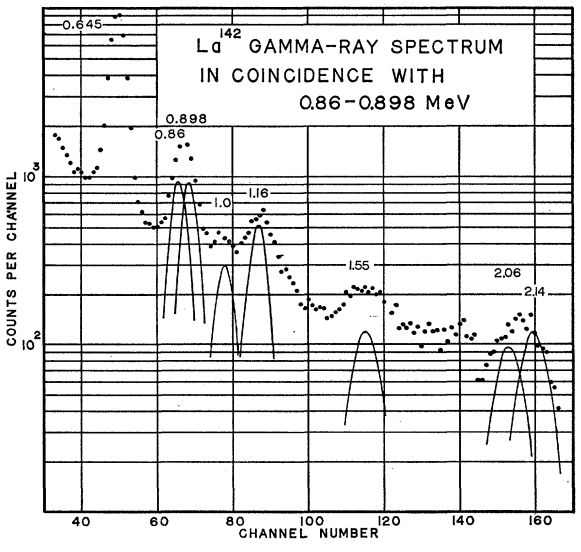

FIG. 4. Spectrum obtained by gating the analyzer with events selected by a 0.05-MeV window centered at 0.88 MeV. For this arrangement $D_{0.898}+D_{0.86}=0.50$.

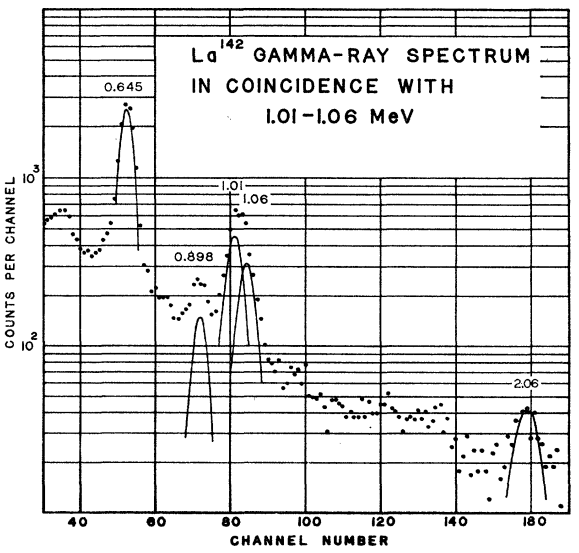

FIG. 5. Pulse-height distribution obtained with a 0.05-MeV window set at 1.03 MeV. $D_{1.01}=0.25$, $D_{1.06}=0.24$.

analysis of the spectrum shown in Fig. 5. This difference reflects the difficulties inherent in the graphical analysis of doublets. The ratio obtained from the spectrum shown in Fig. 6 is believed to be more accurate both because the line shapes used in the analysis were obtained under the same counting conditions and because of the finer mesh resulting from increased gain.

In Fig. 7 is shown the distribution of events in coincidence with gating pulses selected by a 0.06-MeV window centered at 1.25 MeV. For this window setting only 27% of the gating pulses correspond to the 1.25-MeV gamma ray. The most striking feature of the spectrum is the enhancement of the 1.55- and 2.19-MeV peaks. The coincidence-quotient analysis indicates that these transitions are both in coincidence with the 1.25-MeV gamma ray. The coincidences at 2.19 MeV correspond to approximately 80% of the single-crystal intensity so that the doublet nature of this peak appears to be approximately 75% 2.19 MeV and 25% 2.14 MeV.

The intensity of the 1.55-MeV transition in coincidence with the 1.25-MeV gamma ray is 55% of the single-crystal intensity. This is in reasonable agreement with the 0.645-MeV result of 59%. The 1.25- and 0.898-MeV peaks are predominantly due to Compton interference. The 0.645-MeV transition is assigned to be in coincidence with the 1.25-MeV gamma ray on the basis of the analysis.

The gamma-ray spectrum in coincidence with gating pulses selected by a window 0.06-MeV wide centered at 1.55 MeV is shown in Fig. 8. In this spectrum the 1.25-MeV peak is prominent, confirming the existence of the 1.25–1.55-MeV cascade. The coincidence-quotient analysis also confirms the existence of the 0.645–1.55-MeV cascade. The rest of the lines in the spectrum result mainly from gating events not due to the 1.55-MeV transition. This transition comprises only 21% of all the events in the window.

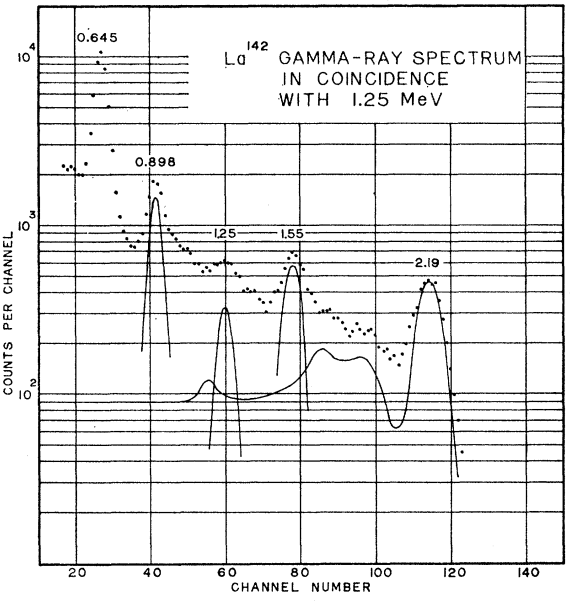

FIG. 7. Coincidence spectrum obtained with a 0.06-MeV window centered at 1.25 MeV. $D_{1.25}=0.27$.

In Fig. 9 is shown the distribution in coincidence with gating events selected with a broad window covering the range 2.0–2.2 MeV. As in the case of the 1.55-MeV coincidence spectrum, the 1.25-MeV line is strongly enhanced, confirming the 1.25–2.19-MeV coincidence relation. The 0.645-MeV line is mainly the result of 2.06–0.645-MeV coincidences. In calculating the coincidence quotients, analysis of the contributions to the window was based on the single crystal and coincidence

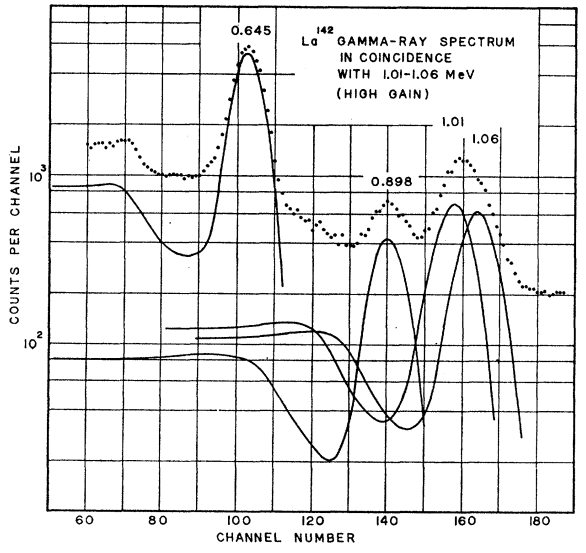

FIG. 6. Low-energy region of the spectrum of Fig. 6, showing the analysis of the 1.01–1.06-MeV doublet.

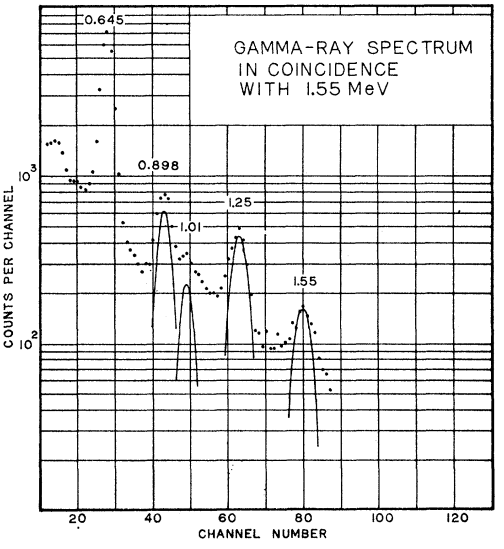

FIG. 8. Coincidence spectrum obtained with a 0.06-MeV window centered at 1.55 MeV. $D_{1.55}=0.21$.

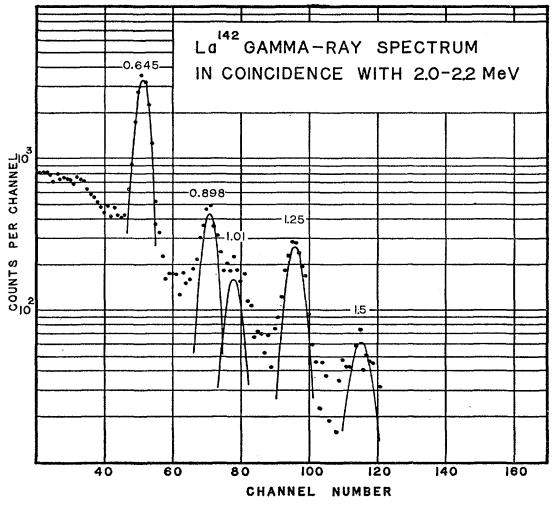

FIG. 9. Pulse-height distribution obtained with a 0.2-MeV window centered at 2.1 MeV. $D_{2.08}=0.25$, $D_{2.14}=0.04$, and $D_{2.19}=0.18$.

data. The gating fractions for the gamma rays of interest are $D_{2.06}=0.25$, $D_{2.14}=0.06$ and $D_{2.19}=0.18$. The corrections for Compton interference were made analytically. In addition, an estimate of the interference was obtained experimentally by comparing this spectrum with the spectrum in coincidence with the window set at 2.5 MeV. The appearance of the 0.898- and 1.55-MeV transitions is further evidence for the coincidence relationships 0.898–2.14 and 1.55–2.14 MeV.

With windows set at the energies 1.74, 1.91, 2.67, and 2.99 MeV, only coincidences with the 0.645-MeV line were identified. The coincidence quotients are given in Table V. The results indicate that these transitions are in coincidence with the 0.645-MeV gamma ray with full intensity to within the expected accuracy of 15%, except in the case of the 2.67-MeV experiment. The errors might be larger than normal in this case since this line is of low intensity and the Compton interference in the window is large.

The low-energy region, 0.5–1.5 MeV, of the spectrum was also measured using the two-dimensional analyzer. In addition to confirming the corresponding results obtained with the fast-slow coincidence spectrometer, the data was also used to obtain the coincidence spectrum correlated with the 1.16-MeV gamma ray. The results confirm the coincidence relationships between the 1.16–0.645- and 1.16–0.898-MeV gamma rays. Other two-dimensional spectra were obtained using various analyzer configurations. The average coincidence-quotient matrix is given in Table II. The summary of relative-intensity measurements based on this matrix and the proposed decay scheme has been given in Table I.

The intensity values obtained from the coincidence data are in relatively good agreement with the values obtained by other methods. The results are expected to have large errors in many instances. The method of coincidence-quotient analysis, because of the successive subtractions involved, tends to accumulate errors. In addition, the higher levels of interference mentioned previously lead to a large dispersion in the results. The average values which combine measurements derived from spectra observed under several different conditions are generally considered to be accurate to 15%.

3.3 Sum-Coincidence Studies

The sum-coincidence spectrum was obtained at a source-to-detector distance of 3 cm. The prominent sum peaks observed in the spectrum are listed in Table III. The individual components of the sum peaks, also given in the table, were determined experimentally. Both the one-dimensional analyzer and pulse-height selector and the two-dimensional analyzer systems were used. When the component sum-coincidence spectra were determined using the two-dimensional analyzer, the sum

TABLE II. La^{142} coincidence quotient matrix.

	Energy of "gating" ray (MeV)														
E_γ (MeV)	0.645	0.86	0.898	1.03	1.16	1.25	1.37	1.55	1.74	1.91	2.06	2.14	2.19	2.67	2.99
0.645			1.05	0.95	0.86	0.63	0.89	0.85	1.2	1.1	0.78			0.62	0.85
0.86	0.04		0.26												
0.898	0.17	1.07		0.03	0.75	0.28		0.24				0.42			
1.01	0.06		0.03	0.97				0.09			0.06				
1.06	0.05		0.02	0.76											
1.16	0.052		0.26												
1.25						0.02		0.39					0.35		
1.37	0.063														
1.55	0.059	0.2				0.47		0.14				0.01			
1.66							0.11								
1.74	0.10														
1.91	0.15														
2.06	0.11		0.08	0.32											
2.14	0.09		0.12												
2.19						0.79									
2.67	0.030														
2.80	0.039														
29.9	0.091														

distribution was assigned to one-dimension and the component spectra to the other. In Fig. 10 is shown the component distribution corresponding to the 1.54-MeV sum peak. The spectrum is seen to consist essentially of only 0.645- and 0.898-MeV components. Interference from the 0.860-MeV transition is reduced as compared to the normal 0.645-MeV coincidence spectrum because of the more selective sum condition. The decay configuration relevant to this sum is also shown in the figure.

Figure 10 also illustrates the component spectrum obtained when a sum energy of 2.06 MeV is selected. In general, the component spectra corresponding to a given sum energy must be comprised of an even number of components. The result shown in Fig. 10 thus confirms the existence of the cascades 0.898–1.16 and 1.01–1.06 MeV, the latter forming a coincidence doublet. The same type of result was obtained for the 0.86–0.898-MeV doublet cascade. In this case the component spectrum consisted of only one peak at an energy of approximately 0.87 MeV when the sum energy 1.74 MeV was selected.

3.4 Beta Transitions

The beta radiations emitted in the decay of La^{142} were studied using the beta-ray scintillation spectrometer discussed above. Each spectrum obtained using this method was corrected for the finite response of the spectrometer. In addition, the single-crystal spectrum was measured with the anticoincidence spectrometer[8] for which only the Gaussian resolution correction was required. Coincidence spectra were measured using the plastic scintillator and a 3-in NaI(Tl) gamma-ray detector in conjunction with the two-dimensional analyzer.

TABLE III. La^{142} summary of sum-coincidence results.

Sum energy (MeV)	Component energy (MeV)
1.54	0.645+0.898
1.72	0.645+1.01, 1.06; 0.898+0.86
2.06	0.898+1.16; 1.01+1.06
2.4	0.645+1.74
2.6	0.645+1.91; 0.645+2.06
3.65	0.645+2.99

In Fig. 11 is shown the single-crystal beta spectrum in the region above 2.5 MeV. The energy calibration was determined using as standard beta sources Cl^{38} (4.81 MeV), Ru^{106}–Rh^{106} (3.53 MeV), Ce^{144} (2.98 MeV), and Sr^{90}–Y^{90} (2.23 MeV). The Kurie analysis of the spectrum, assuming an allowed shape for each component, revealed the existence of beta groups at 4.5 and 3.9 MeV. The experiment was repeated several times using both the anticoincidence spectrometer and the single-crystal arrangement. The spectrum given in Fig. 12 is a composite of the spectra obtained with both methods. It was considered preferable to combine the results from several runs in those cases where insuffi-

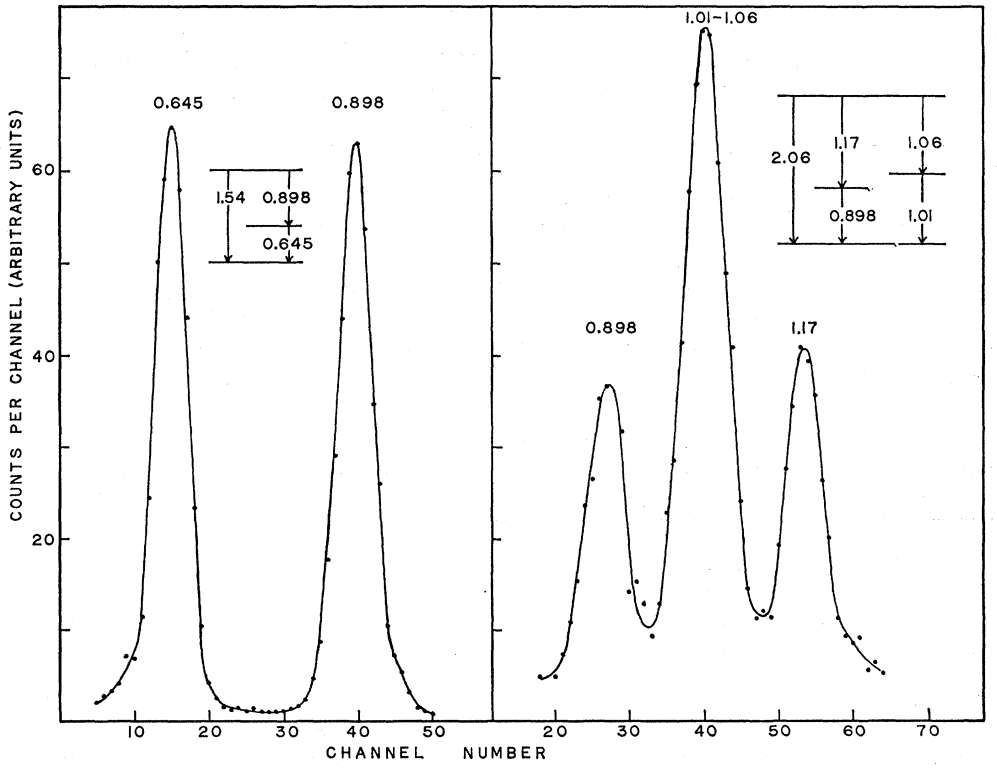

FIG. 10. Component spectra obtained by the sum-coincidence method with sum energies 1.54 and 2.06 MeV. The associated decay configurations are indicated.

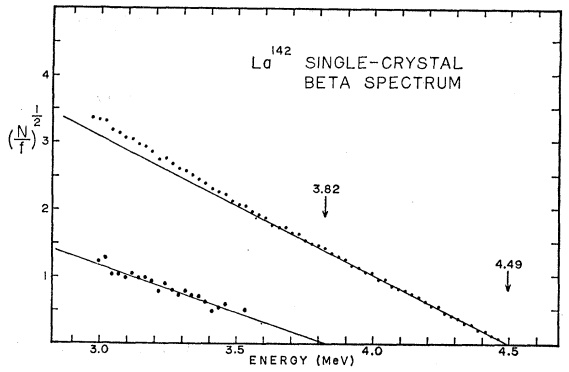

FIG. 11. La^{142} beta spectra above 3 MeV observed with a 2×2-in. NE-102 plastic scintillator. The Kurie analysis of the response-corrected spectrum is indicated.

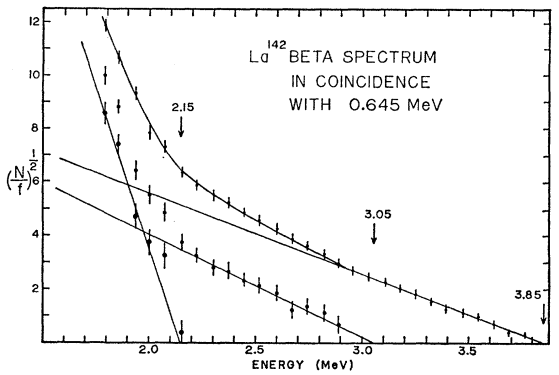

FIG. 12. Kurie analysis of the beta spectrum in coincidence with events selected by a 0.06-MeV window centered at 0.645 MeV. The spectrum shown is a composite of several runs and has been corrected for finite response.

cient counting statistics were obtained rather than to use increased source strength for which significant contributions from random summing occur. Each run was calibrated independently and the channel numbers were converted to energy values. The single-crystal spectra were corrected for finite response. The results were averaged by adding together all the counts in a given energy increment.

A graphical analysis of one entire spectrum obtained with the anticoincidence annulus revealed the existence of the inner groups given in Table IV, as well as a group at 2.41 MeV indentified as the ground-state transition of La^{141}.[3] The coincidence results to be discussed below indicate that not all the groups were revealed in the analysis. In particular, it is believed that the group at 1.8 MeV is in reality an unresolved doublet consisting of the groups β_6 and β_7 and the group at 1.2 MeV is similarly a combination of groups with endpoint energy 1.1 and 1.23 MeV, respectively. The relative intensities of groups revealed in the analysis were obtained by integrating the component spectra. The intensities of the combined groups at 1.8 and 1.2 MeV were assumed to represent the sum of the intensities of the individual components.

In Fig. 12 is shown the beta spectrum in coincidence with events detected in the gamma-ray counter in the energy region corresponding to the 0.645-MeV photopeak. The spectrum shown is a composite of several experiments. The analysis revealed the existence of beta groups with endpoint energies of 3.85, 3.05, and 2.15 MeV. In order to obtain the relative intensities of these groups, it was necessary to make us of the gamma-ray branching ratios and the proposed decay scheme. If r_i is the ratio of the areas of the group β_i to the 3.85-MeV group in the coincidence spectrum, then the branching ratio b_i is given by

$$b_i = r_i \sum_k \frac{f_k}{f_i(1+x)},$$

where the f_k are the relevant gamma-ray branching ratios and x is a first-order correction for Compton interference. In this way the analysis leads to the relative intensities of groups β_2, β_3, and β_5.

In Fig. 13 is shown the spectrum of beta particles in coincidence with events corresponding to the 0.862–0.898 photopeak. Graphical analysis of this composite spectrum reveals the existence of groups at 2.97, 2.1, and 1.7 MeV, identified as groups β_3, β_5, and β_7. The relative intensities of these three groups was determined in the same manner as in the case of the 0.645-MeV coincidence spectrum. For both these spectra the end point of the single-crystal spectrum was used as one calibration point.

In Fig. 14 is shown the beta spectrum in coincidence

TABLE IV. Summary of La^{142} beta groups.

	Singles	0.645	0.898	1.74	1.91	2.06	2.19	2.41	2.55	3.0–3.7	3.65	E	Q_β
β_1	4.49											4.49	4.49±0.04
β_2	3.8	3.85										3.85	4.50±0.05
β_3		3.05	2.97									2.98	4.52±0.05
β_4							2.31					2.31	4.50±0.09
β_5	2.1	2.15	2.10	2.12				2.08				2.11	4.52±0.03
β_6	1.8				1.98				1.96			1.97	4.53±0.06
β_7			1.7			1.84						1.79	4.50±0.03
β_8	1.2									1.23		1.23	4.54±0.09
β_9	0.9									0.86	0.88	0.87	4.52±0.06

$Q\beta = 4.51 \pm 00.3$ MeV.

with events in the 1.91-MeV photopeak. The spectrum was corrected for Compton interference by subtracting the distribution in coincidence with events in the region corresponding to the valley between the 1.91- and 2-MeV photopeaks. The spectrum in this region corresponds to a single group with endpoint 1.98 MeV. The energy calibration was determined using the Compton edges from Mn^{54} and Zn^{65} as well as the standard beta sources. In Fig. 14 is also illustrated the beta spectrum in coincidence with events corresponding to the 2.06–2.19-MeV photopeaks corrected for Compton interference. The analysis reveals groups with endpoint energies 2.31 and 1.84 MeV identified as groups β_4 and β_6, respectively. This spectrum provides the only evidence for the existence of the β_4 group. On the basis of the energies, the β_4 group was assumed to be in coincidence with the 2.19-MeV gamma ray and the β_6 group assigned to be correlated with the 2.06-MeV transition. In Fig. 14 are also illustrated the spectra in coincidence with the 2.41- and 2.55-MeV gamma rays. These spectra consist of single components with endpoint energies of 2.08 and 1.96 MeV identified as groups β_5 and β_6, respectively. The spectrum in coincidence with the 1.74-MeV gamma ray also consisted of a single group of endpoint energy 2.12 MeV corresponding to group β_5. The spectra illustrated in Fig. 14 result from cuts through the two-dimensional distribution of beta-gamma coincidences and were obtained at exactly the same gain and geometry. For this reason the relatively small energy differences between the end points of the spectra are not masked by uncertainties in the calibration.

In Fig. 15 are shown the beta spectra in coincidence with 3.65- and 3.0-MeV events detected in the gamma channel. These spectra indicate the existence of beta transitions with maximum energies of 0.87 and 1.23 MeV. On the basis of the energies and coincidence relations of the gamma-ray transitions, it is believed that the 1.23-MeV group shown in Fig. 15 is in reality an unresolved doublet corresponding to groups with endpoint energies 1.23 and 1.1 MeV.

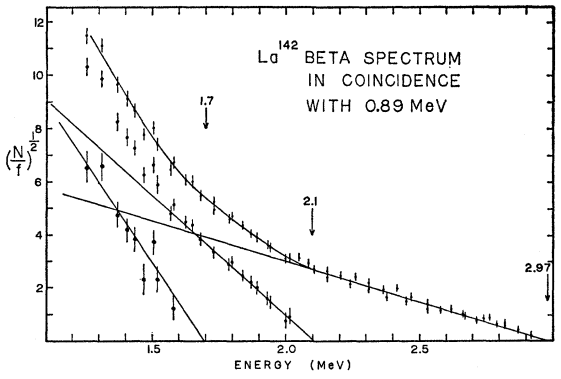

FIG. 13. Kurie analysis of the response-corrected beta spectrum in coincidence with events selected by a 0.07-MeV window centered at 0.88 MeV.

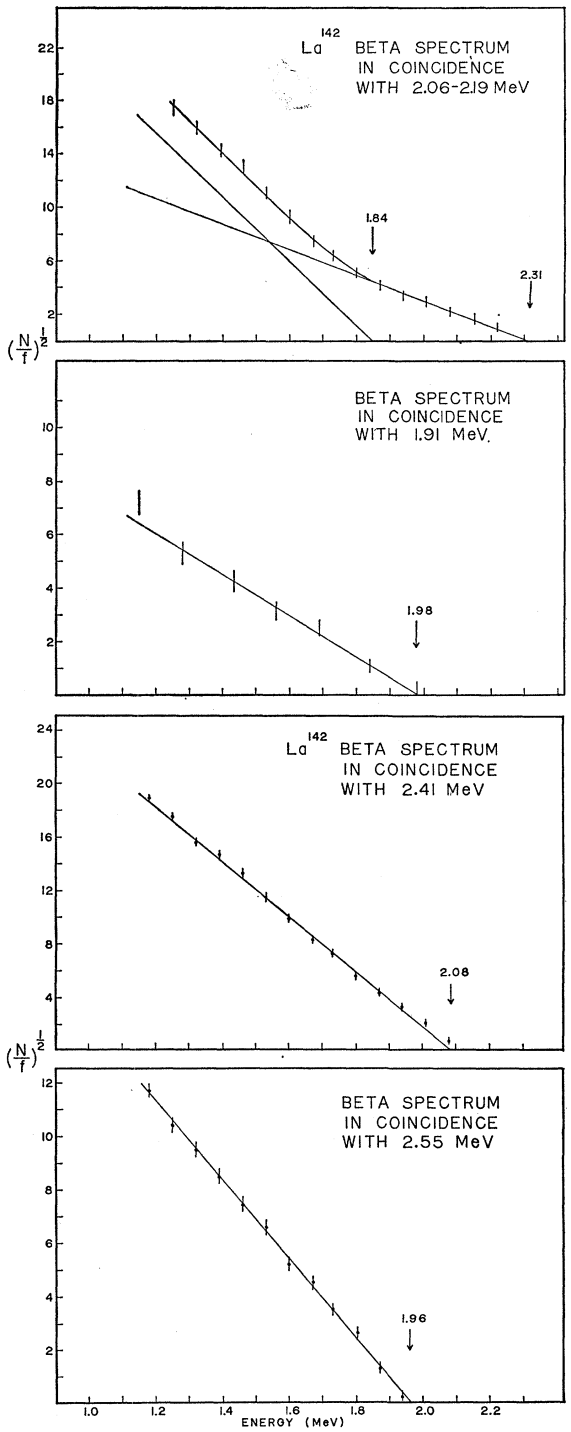

FIG. 14. Kurie analysis of response corrected beta spectra obtained as cuts through the two-dimensional β-γ time correlated distribution. Each spectrum obtains from integration over the indicated photopeaks.

A summary of the evidence for the existence of the nine beta groups observed is given in Table IV. The average value of the endpoint for each groups was determined in those cases for which more than one energy

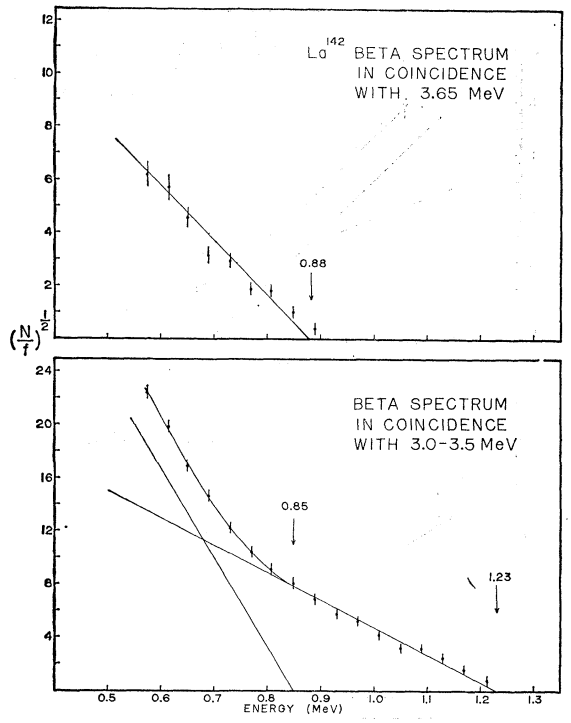

FIG. 15. Kurie analysis of response-corrected beta spectra in coincidence with gamma rays in the energy regions 3.65 MeV and 3.0–3.5 MeV, respectively.

measurement was involved. The value obtained from the endpoint of an inner group revealed by graphical analysis was given less weight in the average than the value obtained under coincidence conditions for which the group under consideration corresponded to the highest energy component. In the case of the beta groups with endpoint energies less than 2.1 MeV, the energy values obtained from the single-crystal spectrum were not included in the average. Also presented in Table IV are the values of the total energy release Q_β. These values are obtained from the energy of the beta group β_i and the average value of the energy of the corresponding level E_i in the proposed decay scheme, based on the gamma-ray energies. The final estimate of Q_β was obtained from the weighted average of the individual measurements.

TABLE V. Intensity of La^{142} beta transitions.

Transition	E_β (MeV)	Intensity (%) Beta measurement	Gamma measurement	Average	Log ft
β_1	4.49±0.05	13	12	12.5	8.9
β_2	3.85±0.04	2.4	3	2.4	9.3
β_3	2.98±0.03	1.7	4	1.7	9.0
	2.5[a]		1	1	9
β_4	2.31±0.05		6.7	6.7	7.9
β_5	2.11±0.03	26	22	24	7.1
β_6	1.98±0.04	20	19	19.5	7.2
β_7	1.79±0.03	11	11	11	7.2
β_8	1.23±0.06	4.4	5.4	4.9	6.9
	1.1[a]	5.6	6.1	5.8	6.8
β_9	0.87±0.03	15	11	13	6.0

[a] The energy of these groups was inferred from the decay scheme.

In Table V are presented the intensities of the beta transitions present in the decay of La^{142} and observed in this work. The relative intensity of the 1.99-MeV group was obtained from the difference between the relative intensities of the combined group revealed in the single-crystal spectrum at 1.8 MeV (31%) and the relative intensity of the 1.79-MeV group obtained from the 0.89-MeV coincidence experiment (11%). The value of the relative intensity for the combined group of 1.2 MeV in the single-crystal spectrum corresponded to 10%. The intensities of the component groups β_8, β_{10} was obtained from the values of the relative gamma-ray intensities, viz.,

$$\frac{I(\beta_8)}{I(\beta_{10})}=\frac{f_{3.31}+f_{2.67}}{f_{3.45}+f_{2.80}}.$$

This formula is based on the proposed decay scheme. The branching ratios were obtained from the relative intensities assuming that these ten groups accounted for 100% of the decays.

The values are compared with the branching ratios obtained directly from the decay scheme and the relative gamma-ray intensities. The values obtained from this method were normalized to those determined from the beta spectra by requiring that the sum of the intensities of the beta groups with endpoint energies less than or equal to 2.1 MeV be the same in both measurements. The branching ratio for the ground-state transition is in this case the difference between the normalized gamma-ray intensities and 100%. The intensities of the groups β_2 and β_3 obtained from the gamma-ray measurements are rather inaccurate since they involve the difference between several gamma-ray intensities. For instance, the intensity of the beta group β_2 results from the difference between the sum of the intensities of ten gamma rays which are believed to populate the relevant level and the intensity of the 0.645-MeV gamma ray.

In principle, a check of the balance between the beta intensities and the intensities of the gamma radiations provides a sensitive test of the validity of a decay scheme. However, the intensities obtained in this work from both beta- and gamma-radiation measurements are not entirely independent. In addition, there is no absolute measurement involved which would verify the assumption that these transitions amount to 100%. The values obtained from both methods do indicate that there is internal consistency in the data within the expected accuracy of the measurements. The final estimates of the branching ratios were obtained by averaging the results obtained from both methods and renormalizing to 100%. In the case of groups β_2 and β_3 the values obtained from the beta measurements alone

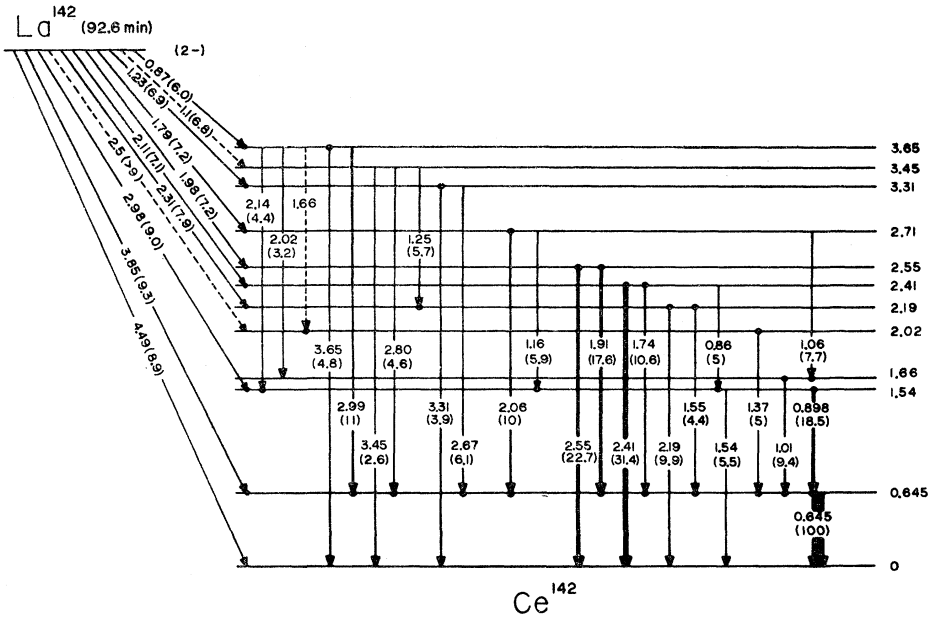

FIG. 16. Proposed decay scheme for 92.6-min La^{142}.

were taken because of the large uncertainty in the values resulting from the gamma-ray intensities.

4. DISCUSSION OF RESULTS

In Fig. 16 is shown a proposed decay scheme for 92.6-min La^{142} constructed on the basis of the experimental results. This decay scheme is consistent with the energies, intensities and coincidence relationships of the beta and gamma radiations observed in this work to within the accuracy of the results. It is believed to account for the prominent deexcitation modes of the La^{142}–Ce^{142} beta decay. Observed coincidence relations are denoted by a full circle, the standard notation of the Nuclear Data Group. The average energy and relative intensity of each gamma ray is given with the intensity in brackets below the energy. The energy and log *ft* value for each beta group are similarly indicated.

The evidence for the first state at 0.645 MeV is conclusive. The 0.645-MeV gamma ray is the transition with the greatest intensity. There are six pairs of gamma transitions, 3.65–2.99, 3.45–2.80, 3.31–2.67, 2.55–1.91, 2.41–1.74, and 2.19–1.54 MeV with energy differences of approximately 0.65 MeV for which the lower energy members were observed to be in coincidence with the 0.645-MeV transition. Finally, the energy difference between the maximum energy beta group observed in coincidence with the 0.645-MeV gamma ray and the ground-state beta transition is approximately 0.65 MeV.

The evidence for the existence of the 1.54-MeV level is based on the strong 0.645–0.898-MeV coincidence and the energy difference between beta groups β_1 and β_3 of approximately 1.5 MeV. The energy of the 1.54-MeV gamma ray indicates that this could be the transition corresponding to deexcitation of this level directly to the ground state. The value of the coincidence quotients $q_{0.645,1.54}$ and $q_{1.54,0.645}$ indicate that approximately half the transitions of this energy occur in coincidence with the 0.645-MeV gamma ray. For this reason the intensity of the 1.54-MeV cross-over transition is only about one half the single-crystal value.

On the basis of energies, previous researchers assigned the 1.01-MeV gamma ray to correspond to a transition between the states at 2.55 and 1.54 MeV. However, the coincidence results obtained in this work give very small coincidence quotients for a 0.898–1.01-MeV time correlation, indicating that these transitions are not incoincidence to the extent required for this interpretation. The strong 0.645- (1.01, 1.06) MeV coincidence requires, therefore, that there be a level at 1.66 MeV. The order of the 1.01–1.06-MeV gamma rays is based on the greater intensity of the lower energy component of the doublet. No beta transition to this level was observed, indicating that it is predominantly populated from the de-excitation of higher energy Ce^{142} states.

The 1.37-MeV gamma transition exhibits coincidence relationships only with the 0.645-MeV gamma ray and a weak 1.66-MeV transition not observed in the single-crystal spectrum. The 0.645–1.37-MeV coincidence was also observed by previous researchers. The 2.02-MeV level included on the basis of this evidence appears to be the only explanation consistent with these results. The evidence for this level is not conclusive, so that it must be considered tentative. No beta group was observed which would correspond to a transition directly to this level.

The relatively strong beta transition with end-point energy of approximately 2.3 MeV observed in coincidence with gamma rays in the energy region 2.0–2.2

MeV indicates the existence of a level at approximately 2.2 MeV. This interpretation is strengthened by the existence of a 2.19-MeV gamma ray and the observation of the 0.645–1.54-MeV coincidence relation. This coincidence was reported earlier; since the existence of the 2.19-MeV gamma ray and the 2.3-MeV beta group was not revealed in the earlier work, it was previously not possible to interpret this coincidence relationship.

The level at 2.41 MeV is required to explain several experimental results. The relatively strong gamma transition at 2.41 MeV exhibits no coincidence relations with other gamma rays. The 0.645–1.74-MeV cascade is then interpreted as resulting from the transition between this level and the first state. Since both the 2.41- and 1.74-MeV gamma rays are in coincidence with the same group with endpoint energy 2.1 MeV, the interpretation is consistent with the beta-gamma coincidence results. Finally, the existence of the 0.86–0.898-MeV doublet and the appearance of the β_5 group in coincidence with gamma rays in the region of 0.645 and 0.898 MeV requires that the 0.86-MeV gamma ray correspond to the transition between the 2.41-MeV level and the second state.

The evidence for the existence of the 2.55-MeV level is based on the appearance of the 2.55-MeV gamma ray uncorrelated with any other transition. This property indicates that the transition results from a de-excitation leading directly to the ground state. The 0.645–1.91-MeV coincidence indicates that the 1.91-MeV gamma ray corresponds to the transition between the 2.55-MeV level and the first state. This interpretation is confirmed by the fact that both the 2.55- and 1.91-MeV gamma rays are in coincidence with the β_6 group and therefore depopulate a common level at approximately 2.6 MeV. The coincidence quotients for a possible 0.898–1.01-MeV cascade indicate that if a transition exists between this level and the second state, it can represent at most a 2% branching ratio for the de-excitation of the 2.55-MeV level.

The presence of the 1.8-MeV beta group indicates the existence of a level at approximately 2.7 MeV. This group appears in coincidence with gamma rays in the region of 2.0 MeV. This result, together with the fact that there exists a 2.06-MeV gamma ray in coincidence with the 0.645-MeV gamma ray is consistent with the interpretation that the 2.06-MeV gamma ray corresponds to the transition from the 2.7-MeV level to the first state. The 0.898–1.17- and 1.01–1.05-MeV cascades appear as components of the 2.06-MeV sum-coincidence peak so that the 2.06-MeV transition is interpreted as the cross-over transition for these cascades. Finally, the observed coincidence relationship between the 0.898-MeV gamma ray and the β_7 group indicates that the 1.17-MeV gamma ray corresponds to the de-excitation of this level leading to the second state. No transition from this level to the ground state was observed. It is estimated on the basis of the regression analysis of the single-crystal spectrum that the branching ratio for such a transition must be less than 3%.

The level at 3.31 MeV is based upon the identification of a 3.31-MeV gamma ray exhibiting no coincidences with other gamma rays and a 1.2-MeV beta group observed in coincidence with a gamma ray of energy greater than 3 MeV. The observed 2.67–0.645-MeV coincidence is consistent with the identification of the 2.67-MeV gamma ray as corresponding to the transition between this level and the first state. No other de-excitation modes for this level were positively identified.

The existence of a level at 3.45 MeV is required by the observed properties of the 3.45- and 2.8-MeV gamma rays. The 2.8-MeV gamma ray was observed to be in coincidence with the 0.645-MeV transition. In addition, the 2.19–1.25- and 1.54–1.25-MeV coincidences are consistent with the identification of the 1.25-MeV gamma ray with the transition between the 3.45- and 2.19-MeV levels. The beta group corresponding to the population of the level following the decay of the La^{142} ground state was not observed. It is felt that the energy of this group of approximately 1.1 MeV is sufficiently close to that of the 1.2-MeV group so that under the counting conditions used in this study these two groups were not resolved. The existence of this group was inferred from consideration of the relative gamma-ray intensities. As in the case of the 3.31-MeV level, no transitions leading to levels other than those indicated were positively identified.

The highest energy gamma ray observed in the La^{142} spectrum at 3.65 MeV is in coincidence with the lowest energy beta group identified at approximately 0.9 MeV. Since this gamma ray was not observed in coincidence with any other transition, it may be interpreted as the ground-state transition of a level at 3.65 MeV. This interpretation is consistent with the beta-gamma coincidence results and with the relatively strong 0.645–2.99-MeV coincidence. The 0.898–2.14- and 1.03–2.02-MeV coincidences indicate that these two gamma rays at approximately 2 MeV correspond to de-excitation modes for which the final levels are the 1.54- and 1.66-MeV levels, respectively.

The decay scheme presented accounts for all the observed beta and gamma transitions and their interrelations. The residual which occurs in some coincidence spectra may indicate that other de-excitation modes of low probability occur in the beta decay of La^{142} in addition to those identified in this study.

On the basis of the relative gamma-ray intensities and the branching ratios of the beta groups, the absolute intensity of the 0.645-MeV gamma ray was calculated to be $50\pm5\%$. This value is in reasonable agreement with that measured by Schumann *et al.*[3] of approximately 55%. No error is quoted by these authors.

The average value obtained for the total energy release, 4.51±0.03 MeV, is consistent with the systematics of disintegration energies in this mass region[10] and is in good agreement with the previously measured value of approximately 4.4 MeV.[3] No estimate of the accuracy of the previous measurement is given by the authors, but an arbitrary error of 0.3 MeV was assigned by the Nuclear Data Group.[10]

PHYSICAL REVIEW VOLUME 134, NUMBER 3B 11 MAY 1964

Properties of Gamma Transitions in the Decays of Sm^{153} and Gd^{153} into Eu^{153}†

PETER ALEXANDER
California Institute of Technology, Pasadena, California
(Received 18 December 1963)

The energies and relative intensities of gamma rays produced in the electron-capture decay $Gd^{153} \rightarrow Eu^{153}$ and of the low-energy gamma rays produced in the beta decay $Sm^{153} \rightarrow Eu^{153}$ have been studied with the bent-crystal spectrometer. Two previously unreported gamma rays have been observed at 54.19 and 68.23 keV. These together with a previously reported 151.5-keV gamma transition depopulate a new state at 151.61 keV which we propose as the $\frac{7}{2}^-$, $K=\frac{5}{2}$ level of Eu^{153}. The $M1$ gamma-ray interband branching ratio from the known 173-keV $\frac{5}{2}^+$, $K=\frac{3}{2}$ level and the $E1$ gamma branching ratio from the 151.61-keV level are examined for evidence of band mixing.

INTRODUCTION

THE decays of Sm^{153} and Gd^{153} into Eu^{153} are known to involve three clearly identified intrinsic configurations. These are the $K=\frac{5}{2}^+$ [413] ground-state band, the $\frac{5}{2}^-$ [532] intrinsic level at 97 keV and the $K=\frac{3}{2}^+$ [411] band at 103 keV. A number of conversion-electron lines attributed to decays from a series of unclassified levels in the region 630 to 710 keV have been previously reported.[1,2] In Fig. 1 we present a scheme for the decays of Sm^{153} and Gd^{153} into Eu^{153}. This scheme incorporates the results of some earlier works as well as the new information obtained from the present investigation.

Properties of the excited states of Eu^{153} are of particular interest because of the location of this nucleus at the border of the region of strongly deformed nuclei. Mottelson and Nilsson have been rather successful in interpreting the properties of this decay in terms of the collective model.[3] The apparent change of eccentricity between the [413] and [411] bands on the one hand and the [532] band on the other renders interesting information concerning transitions between these bands.

Various groups have studied the Sm^{153} and Gd^{153} decays examining both internal-conversion and gamma-ray spectra.[1,2,4–8] Recently, Suter *et al.*[2] have made an extensive investigation of the Sm^{153} decay using internal-conversion measurements to obtain transition energies and external-conversion data for gamma-ray intensity values. At present there exists no comprehensive direct measurement of the Eu^{153} relative gamma-ray intensities while there is some contradiction in the intensity data for those gamma rays which have been studied.[4,5,8] A number of weak but unassigned conversion electron lines in the decay from Sm^{153} have been reported.[2]

We have made an accurate determination of the relative gamma-ray intensities in the Sm^{153} and Eu^{153} decays. In addition, we have established a previously unobserved rotational level at 151.61 keV. This level is depopulated by a previously reported[2] 151.5-keV gamma ray and two previously unreported gamma rays at 54.19 and 68.23 keV. A search of the low-energy gamma-ray spectrum failed to reveal any additional gamma rays which might be associated with the several weak but unassigned electron-conversion lines reported in Ref. 2.

SOURCES

Our sources were prepared by encapsulating Sm^{152} (enriched to 99.06%) and Gd^{152} (enriched to 95%) separately in quartz capillaries. These capillaries had

† Work performed jointly under the auspices of the U. S. Atomic Energy Commission and the National Science Foundation.
[1] V. S. Dubey, C. E. Mandeville, and M. A. Rothman, Phys. Rev. **103**, 1430 (1956).
[2] T. Suter, P. Reyes-Suter, S. Gustafsson, and I. Marklund, Nucl. Phys. **29**, 33 (1962).
[3] B. R. Mottelson and S. G. Nilsson, Kgl. Danske Videnskab. Selskab, Mat. Fys. Skrifter **1**, No. 8 (1959).
[4] C. W. McCutchen, Nucl. Phys. **5**, 187 (1958).
[5] R. E. Sund and M. L. Wiedenbeck, Phys. Rev. **120**, 1792 (1960).
[6] R. L. Graham, G. T. Ewan, and J. S. Geiger, Bull. Am. Phys. Soc. **5**, 21 (1960).
[7] E. Monnand and A. Moussa, Nucl. Phys. **25**, 292 (1961).
[8] L. Block, W. Goedbloed, E. Mastenbroek, and J. Block, Physica **28**, 993 (1962).